

Effects of alendronate in bone repair: A study in rat femur fractures treated with plates and screws

Fernanda Tiboni

Universidade Positivo <https://orcid.org/0000-0002-2511-8019>

Suyany Gabriely Weiss

Universidade Positivo

Jennifer Tsi Gerber

Universidade Positivo

Arieli Carini Michels

Pontificia Universidade Catolica do Parana

Thais Grupp da Rosa

Pontificia Universidade Catolica do Parana

Thaís Costa Casagrande

Universidade Positivo

Tatiana Miranda Deliberador

Universidade Positivo

Allan Fernando Giovanini

Universidade Positivo

Aline Cristina Johann

Pontificia Universidade Catolica do Parana

Rafaela Scariot (✉ rafaela.moraes@up.edu.br)

Research article

Keywords: alendronate, bisphosphonates, bone regeneration, fracture, femur, TGF beta-

Posted Date: June 26th, 2020

DOI: <https://doi.org/10.21203/rs.3.rs-33681/v1>

License:   This work is licensed under a Creative Commons Attribution 4.0 International License.

[Read Full License](#)

Abstract

Background

Alendronate (ALN) has direct action on bone metabolism, increasing osteogenesis and decreasing bone resorption. The study rated the effect of ALN on femoral fracture repair and the effect of different doses of the drug on the liver and kidneys.

Methods

Wistar rats were divided into groups: A1 (ALN 1 mg/kg), A2 (ALN 3 mg/kg), and C (saline solution). The drug/solution was applied intraperitoneally three times a week after femoral fracture until euthanasia 45 days later.

Results

Liver analysis from group A1 presented normal histological aspects, while hepatic steatosis was observed in group A2. In groups A1 and A2, kidneys showed amylocymile like cell degeneration. In femur bone callus, no difference was observed in collagens I and III or in number of trabeculae ($p \geq 0.05$). Immunohistochemical evaluation showed positivity for the Transforming Grow Factor β -1 (TGF β -1) marker in the control group, in spinal area and in small chondrocytes, but negativity for hypertrophy. In A1, an extensive area of cartilaginous expansion was observed, with positive hypertrophic TGF β -1 cartilage, even in areas with bone matrix. A low positivity was observed in the medullar area, in contrast to the control. Group A2 presented a high number of chondroid matrices and a moderate number of TGF β -1 cells, with little positivity in medullary area.

Conclusions

A dosage of ALN 1 mg/kg promotes cellular differentiation activity in the bone callus region, with mild damage in the liver and kidneys. A dosage of ALN 3 mg/kg became toxic without positive alterations in cell differentiation.

1 - Background

Bisphosphonates are drugs with the potential to stimulate osteogenic action or to reduce bone resorption activity, and they are an ally in the process of bone fracture consolidation (1). Within this class of drugs, the most prescribed is alendronate sodium (ALN), a second-generation amino bisphosphonate that is a potent inhibitor of osteoclastic absorption. The use of ALN causes a decrease in osteoclastic activity without directly interfering in neof ormation: the drug is quickly distributed to bones or excreted by kidneys (2, 3). Alendronate acts directly on Transforming Grow Factor β -1 (TGF- β 1) by increasing its amount,

which induces osteogenesis and chondrogenesis, which in turn play an important role in cell growth, differentiation, and protein synthesis of the extracellular matrix (4–6).

When a fracture occurs, a complex consolidation process begins, one that involves several cells and signaling molecules. The new bone is formed by mesenchymal osteoblasts derived from progenitor sites. Osteoclasts from circulation and hematopoietic precursor cells migrate in order to digest old bone. During bone remodeling, catabolic and anabolic activities interact; both of these reactions can be modulated by drugs (7–10). It is this phase that would benefit from the use of substances such as ALN, which have the potential to stimulate osteogenic action, reduce bone resorption activity, and assist in the consolidation process (1, 11–13). When combined with anabolic-active drugs, ALN significantly improves bone mineral density and reduces bone fracture (3, 8, 14, 15). Previous research has shown that short-term ALN treatment also improves bone repair around implants installed in the tibias of osteoporotic rats, demonstrating the drug's potential therapeutic effect (16, 17).

Furthermore, during the scarring process in the inflammatory phase, some growth factors—such as TGFs—are constantly in action. Among TGFs, TGF- β 1 has direct effects on the regulation of osteoblast differentiation (18). ALN acts on this marker, increasing the amount of TGF- β 1 and consequently the cell migration that increases the matrix. This leads to a higher number of bone trabeculae and smaller distances between them (5, 6), suggesting that ALN treatments increase the strength and stiffness of fractured bones (8).

ALN has a high potential to increase bone mineral density, but information is lacking regarding ideal experimental ALN doses and time of post-operative administration for ideal bone repair. Therefore, the aim of this study is to demonstrate the effect of alendronate sodium on femoral fracture repairs and the effect of different doses of this drug on the kidneys and liver.

2 - Methods

2.1 - Ethical considerations

The experiments were carried out at the histology laboratory and in the Bioterium of Positivo University with animals provided by the same bioterium and was approved by the Ethics Committee on Research and Animal Use (Protocol ECAU 320). The entire procedures with animals, followed the ARRIVE guidelines (Supplementary File). Throughout the experiment, the ambient conditions of the rooms were controlled by a digital panel, including humidity (65%), light (photoperiod of 12 hours) and temperature (18 to 22 degrees Celsius).

2.2 - Experimental design

Were used a total of 45 male Wistar rats (*Rattus norvegicus*), weighing approximately 500 grams and 5 months old, they were randomly divided equally into 3 groups: group C (control), group A1 (1 mg/kg of ALN), and group A2 (3 mg/kg of ALN). During the experimental period, all animals were assigned in

identified cages with maximum 3 rats per cage. Seven animals were lost during surgery or the postoperative phase (Fluxogram 1). Intraperitoneal applications of ALN were initiated on the opposite side of the fracture surgical procedure. Control group received applications of 0.9% saline solution. The application was maintained in a frequency of at 3 times a week until the euthanasia, 45 days after the surgical procedure.

2.3 - Surgical procedure

The rats were sedated for 1 minute via inhalation of isoflurane (Cristália, Itapira, SP, Brazil) and after anesthetized by intramuscular injection with 10% ketamine hydrochloride (Vetbrands, Paulínia, SP, Brazil) and 2% xylazine hydrochloride (Vetbrands, Paulínia, SP, Brazil). Under anesthesia, the animals were placed in the left lateral decubitus position, and then the right pelvic member was surgically exposed and the surgery developed according to the technique described by Weiss *et al.* (16). A 5 cm straight incision was made with No. 15C blade along the long axis of the femur; blunt scissors and hemostatic tweezers were used for tissue divulsion, that way the muscle was separated into plans. Next, was incised the periosteum with a scalpel and detached with a delicate syndesmotome, allowing access to the cortical surface of the femur.

Before the osteotomy, it was necessary to keep the bone position, drill, and adapt the 2.0-mm 4-hole titanium plate system with four 4-mm screws, in order to avoid poor positioning of the segments. The fracture was then performed with the NSK™ Reciprocating Saw (NSK™ Shinagawa, Tokyo, Tokyo, Japan). Analgesia (tramadol, 7 mg/kg twice a day for 5 days), inflammation (ketoprofen, 5 mg/kg once a day for 5 days), and infection (enrofloxacin, 10 mg/kg once a day for 7 days) were controlled in the postoperative period.

2.4 - Euthanasia

All animals were euthanized after 45 days with an overdose of isoflurane. Kidneys, livers, and femurs were removed and stored in a 10% formaldehyde solution for preservation. The pieces were subsequently processed and maintained in paraffin blocks. The blocks were sectioned longitudinally in serial 3- μ m sections for histological analysis of the visceral parts and for histomorphometric and immunohistochemical analyses of the femur. Due to postoperative infection and/or fracture of the femur, three rats were euthanized prematurely (within the seven-day postoperative period) to prevent suffering. Two animals experienced a not adequate fracture femur during surgery, probably due to the size of the bone in those rats. These rats were euthanized immediately. One rat was considered lost because the sample was lost after euthanasia when the plate and screws were removed.

2.5 - Histological analysis: Liver and kidneys

The kidneys and livers were longitudinally hemisected and then stained with hematoxylin and eosin (HE) and were analyzed by light microscope (021/3 Quimis, Diadema, SP, Brazil), in which the following parameters were evaluated: cell morphology, cellular disposition, and degree of normality.

2.6 - Histological analysis of collagen: Femur

The specimens were processed histologically and stained by picrosirius staining, according to standard routine procedures. The slides were digitized in the ZEN program (ZEISS™ Microscope Software ZEN Lite). For the analysis, a single observer captured 10 images per slide in the region of the bone callus, with a magnification of 200×. The images were analyzed in the Image Proplus™ 4.5 (Media Cybernetics, Silver Spring, MD) morphometry program, which automatically measured the areas and percentages of type I (mature collagen) collagen fibers, type III (immature) collagen fibers, and total collagen fibers, expressing these findings in square micrometers (μm^2). The statistical means of each rat were obtained. In contrast to a black background, type I collagen fibers were considered to have red-orange coloration, and type III collagen fibers were considered to have yellow-green coloration.

2.7 - Histomorphometric analysis: Femur

The tissue sections of the decalcified and HE-stained femurs were analyzed by light microscopy (Olympus™ BX41, Melville, NY, USA) with a magnification of 100x and were photographed serially with a digital camera (EOS Rebel T5, Canon, Japan). With an Image J™ program (version 1.49t National Institute of Health-NH, Bethesda, MD, USA), the histomorphometric measurements of the total area, along with the internal and external areas of bone callus trabeculae, were performed in pixels (see Fig. 1). In order to evaluate the reliability of the measurements, the data obtained from part of the sample were measured at different times by the same operator (ICC-95%: 0.98).

2.8 - Immunohistochemical analysis: Femur

The tissue sections of the decalcified femurs were dewaxed with xylol and progressively rehydrated with a solution of 100 – 70% ethanolic gradient, water, and 1% sodium phosphate. Antigen retrieval was performed for 60 minutes at 37 °C by contact with a solution of pepsin – 1N (pH 7.2). The slides containing the histological sections were immersed in hydrogen peroxide in a dark chamber. After 15 minutes, the reaction was blocked by adding milk protein concentrate. The sections were incubated for 18 hours with the primary antibody TGF- β 1 (Santa Cruz Biotechnology™, Inc. 10410 Finnell Street Dallas, Texas 75220, USA), with a 1:200 dilution factor. Reactions were revealed with the use of 3,3-diaminobenzidine tetrachloride (Sigma™, St Louis / USA) for 3 minutes, resulting in a brownish staining at the antigen site. The sections were counterstained with Harris Hematoxylin.

2.9 - Statistical analysis

The original count of 45 rats was used to maintain a statistically valid sample per group. Results were given over to descriptive and statistical analysis. The collagen measurements were compared across groups by one-way ANOVA test. The measurements of the histomorphometric analysis were classified as non-parametric. The difference between groups was analyzed by the Kruskal-Wallis test. Statistical evaluation was performed using the Statistical Package for Social Science (SPSS), version 24.0 (SPSS Inc.™ Chicago, IL - USA), with a 95% confidence interval.

3 - Results

3.1- Histological analysis: Livers and kidneys

Histological analysis was performed on the livers (Fig. 2A) and kidneys (Fig. 2D) of the control group to ensure normality and absence of morphological changes. The analysis shows livers with an abundance of patent capillaries and sinusoids, as well as kidneys with normal proximal and distal conduits and well-formed glomeruli.

The livers of group A1 (Fig. 2B) presented a normal histological aspect, with no metabolic alterations, a normal portal area, polygonal cells with normal portal space, and a lobular internal area without alterations. As for the livers of group A2 (Fig. 2C), it was possible to notice the presence of hepatic cells with a clear cytoplasm of a guttular nature, characteristic of hepatic steatosis. Fat areas among cells were also observed.

The renal analysis of group A1 (Fig. 2E) showed well-formed glomeruli, intense afferent vessels, proximal and distally-contorted ducts, morphologically normal and normal cortical. Cells showed amylocymile-like degeneration, and medullary alteration. Group A2 (Fig. 2F) showed intact cortical kidneys, with no change in the filtration metabolism in the distal convoluted tubule and collecting tube. The cells showed amylocymile-like degeneration, with ballooned cells, which may indicate some disturbance in the metabolism of the neoglucogenesis.

3.2 - Histological analysis of collagen: Femur

In table I, one can see the values of collagen I and collagen III in all three groups. No difference can be found among the groups ($p > 0.05$).

3.2 - Histomorphometric analysis: Femur

The values obtained after decreasing the total area of the image and the area of medullary space are shown in Table II. Comparisons of the median values of each group show no statistical differences among them, for the internal callus ($p = 0.7850$) or for the external callus ($p = 0.5982$).

No difference was found when the amount of bone in the internal callus was compared with the amount of bone in the external callus ($p = 0.182$).

3.3 - Immunohistochemical analysis of femur

The control group (Fig. 3A) demonstrated positivity for the TGF- β 1 marker and the predominant marking in the marrow area, which is inserted in the area of bone formation. Positive markings were also observed on small chondrocytes despite negativity for hypertrophic cells, appearing in small quantities. In group A1 (Fig. 3B), an extensive area of cartilaginous expansion was observed, dominated by hypertrophic cartilage and TGF- β 1 cells, even in areas containing bone matrix. Low positivity was observed for the marker in the medullar area, in contrast to the control group. In group A2 (Fig. 3C), the high amount of chondroid matrix can be seen in the middle of the hypertrophic cartilage and a moderate number of TGF-

β 1 cells. Low positivity for the marrow marker completes the frame, demonstrating that higher ALN concentration brings lower TGF- β 1 labeling.

In Table III, it is possible to see the immunostaining of TGF- β 1 in different regions, according to group.

4 - Discussion

This article presents two important main findings; one is the effects of ALN on the liver and kidneys after using alendronate in bone repair. These two organs had been chosen due to their direct relation with the drug. Glucocorticoids are metabolized by the hepatic route, and they are involved in the suspension of bone formation and the promotion of bone resorption, inducing osteoporosis. The kidney evaluation was important because this organ is responsible for ALN excretion (17).

As far as systemic involvement is concerned, many studies (2,5,13,12,18–24,) have used this type of drug at different dosages and concentrations (aiming to accelerate bone repair) without evaluating the general health implications since the ALN had a nonlinear uptake by bone, accompanied by simultaneous accumulation in noncalcified tissues at high doses (25). This study has shown that the treatment with 3 mg/kg of ALN significantly increases liver and kidney damage compared to a placebo. A dose of 1 mg/kg could be used therapeutically in humans, as its effects are not as serious as a dose of 3 mg/kg. A study by Erlebacher *et al.* (26) examining collapsed focal segmental glomerulosclerosis in a patient receiving liver transplantation due to alendronate use for osteopenia—concluded that the drug was not related to renal toxicity at a dose of 0.3 mg/kg. However, it should be emphasized that bisphosphonates must be used with caution in patients with low glomerular filtration rate (27).

A previous study observed that a dose of 3 mg/kg caused systemic alterations in animals, with hepatic impairment (28). In Deliberador *et al.* (15) work, local applications of 1 mg/kg alendronate in rat calvaria defects were delivered, the authors concluded that the kidneys showed normal glomeruli, with capillaries surrounding these structures. No impact on the kidneys was observed in any group of their work. This study did not analyze blood biochemistry, which is an important indicator of possible future systemic complications. Li, F *et al.* and Srisubut *et al.* had also studied the effects of local delivery of ALN and suggest that the drug have increased bone formation (29, 30). Wang, YH *et al.* linked PLGA (lactic-co-glycolic acid) to ALN for slow and local application and found an excellent graft potential (31).

The second main finding is the effect of different doses of alendronate on bone repair. We chose to use the human-based dose, which corresponds to 1 mg/kg, as well as a dose triple that. Previous research has already shown that reduced doses of alendronate may improve osteoblast differentiation and bone matrix formation (25, 32), although the literature has not expounded on whether the ideal dosage of the drug can benefit bone repair. A greater dosage of ALN has been proven to be more effective in qualitative microtomographic analysis of bone repair. This could be seen through the greater number of trabeculae and the decreased spacing between the trabeculae in the 3 mg/kg group (6, 16, 33). More bone density suggests that a higher dosage influences bone quality, which encouraged the researchers in this experiment to use both 1 mg/kg and 3 mg/kg.

Types I and III collagen are the main collagens found in the connective tissue matrix. Type I can be found in tendons, fibrous cartilage, and bone (among others); type III can be found in a wide range of tissues, varying from spleen to granulation tissue, and it plays a special role in tissue regeneration, given the early increase in its expression following tissue injury (34). Reduced collagen III has been demonstrated to decrease bone formation and remodeling alterations during fracture healing. In 2015, Miedel *et al.* (35) showed that collagen III levels begin to increase in the first two days following a long bone fracture and remain elevated for the first three weeks; the collagen can be found throughout immature woven bone of murine fracture callus, although it is less prevalent (by comparison) in the cartilaginous matrix. ALN act increasing bone volume and the level of mature collagen I reserve (36). That data suggests that collagen III is less likely to play a significant role in endochondral ossification, which might explain why the researchers of this study could not find significant differences among groups in terms of the time of euthanasia and callus remodeling.

In terms of quantitative effect on bone repair, in this study no correlations were found between doses and area of trabecular bone in the femur. One hypothesis is the duration of drug delivery. The researchers believe that a longer time period (more than 45 days) is critical. A study of dose-response relationship for ALN treatment in elderly osteoporotic women showed that treatment with ALN (1, 2.5, or 5 mg/day) decreased bone absorption markers and reduced markers of bone formation in a dose-related but delayed manner, with all doses evaluated (27). Study of Ramchand *et al.* shown that a chronic use of BF, decrease the bone remodeling as the bone volume (37).

Another hypothesis for no association is that alendronate was only used after the surgical period. Other studies show pre-surgery use, both with and without success. Wan Rong *et al.* (38) had a total of 82 osteoporotic patients whose humerus fractures were stabilized with plaques. They divided the sample into two groups: group A (initiation of bisphosphonate treatment within two weeks after surgery) and group B (control group, initiation of treatment three months after surgery). They concluded that all patients had fracture union, and the mean time to radiographic union was similar in groups A and B.

Another important point of this study was the choice of the TGF- β 1 marker to accomplish the immunohistochemical evaluation. This marker is responsible for maintaining a constant bone mass, acting directly on the regulation of osteoblast differentiation and promoting polymorphonuclear cell chemotaxis, fibroblast proliferation, and collagen I synthesis (5). TGF- β 1 is a physiological regulator of osteoblast differentiation and a key mediator of the coupling of osteoblast differentiation and osteoclastic bone resorption, which is required for skeletal homeostasis (26). Study of Vieira JS *et al.* demonstrated that ALN influences marker TGF- β 1 changing the production and remodeling of the chondroid extracellular matrix (39). Other studies had also proved the relation between them, suggesting that ALN acts directly on this marker, increasing its level (5, 6) A smaller dosage of ALN (1 mg/kg) contributed with less negative impact on the TGF- β 1 marker compared to the higher dosage (3 mg/kg), as noted in this study. A study by Jei *et al.* (5) concluded that prolonged reduction of bone turnover after alendronate treatment in female rats increased TGF- β 1 production by bone marrow cells and periosteal osteoprogenitors.

5 - Conclusion

In terms of increasing bone repair in fractured bones, a dosage of 1 mg/kg ALN showed better activity on the bone callus of cellular differentiation with less impairment of the liver and kidneys. A dosage of 3 mg/kg ALN became toxic, with significant damage to the liver and kidneys.

6 - Declarations

Ethics Approval and Consent to participate

Approval by the Ethics Committee protocol number 320, ECAU – Positivo University, Curitiba, Paraná, Brazil

Consent Publication

Not applicable

Availability of Data and Materials

Not applicable

Competing interests

The author declare that they have no competing interests.

Funding

None

Author's Contributions

FT performed most of the surgical experimental procedures and post-operative follow up, described their result appointments and as well drafting the manuscript. **SGW** participated in the surgeries and in the post-operative follow up as also reviewing the manuscript. **JTG** was responsible for the post-operative agenda, medicating animals and controlling feeding, room temperature and cage cleaning. **TGR** responsible by collagen analysis. **ACM** responsible by the collagen table. **TMD** supervising the surgical procedures. **AFG** responsible by the immunohistochemical and histomorphometrical analysis. **ACBRJ** did the collagen reading sheets. **RS** as the group leader, gave the guidelines for the whole project execution. All authors have read and approved the manuscript.

Acknowledgements

Authors would like to thank the Positive University for providing the Histology Lab and the bioterium that made this study possible.

Abbreviations

ALN – Alendronate sodium

TGF β -1 – Transforming Grow Factor β -1

ECAU – Ethics Committee on Research and Animal Use

A1- Alendronate 1mg/kg group

A2 – Alendronate 3mg/kg group

C – Control group

PLGA – Lactic-co-glycolic acid

References

1. Greiner SH, Wildemann B, Back DA, Alidoust M, Schwabe P, Haas NP, et al. Local application of zoledronic acid incorporated in a poly(D,L-lactide)-coated implant accelerates fracture healing in rats. *Acta Orthop*. 2008;79(5):717-25. DOI: 10.1080/17453670810016768
2. Haddad PT, Salazar M, Hernandez L. Histomorphometry of the organic matrix of the femur in ovariectomized rats treated with sodium alendronate. *Revista brasileira de ortopedia* 2015;50(1):100-104. DOI: 10.1016/j.rboe.2014.12.007
3. Molteni R. Prospects and challenges of rendering tissue density in Hounsfield units for cone beam computed tomography. *Oral Surg Oral Med Oral Pathol Oral Radiol*. 2013;116(1):105-19. DOI:10.1016/j.oooo.2013.04.013.
4. A. Guermazi, G. Kalsi, J. Niu, M. D. Crema, R. O. Copeland, A. Orlando, et al. Structural effects of intra-articular TGF- β 1 in moderate to advanced knee osteoarthritis: MRI-based assessment in a randomized controlled trial. *BMC Musculoskelet Disord*. 2017; DOI 10.1186/s12891-017-1830-8. DOI: 10.1186/s12891-017-1830-8
5. Jei J, Yao W, Amugongo S, Shahnazari M, Dai W, Lay YE, et al. Prolonged Alendronate Treatment Prevents The Decline In Serum TGF- β 1 Levels And Reduces Cortical Bone Strength In Long-Term Estrogen Deficiency Rat Model. *Bone*. 2013;52(1):424-32. DOI: 10.1016/j.bone.2012.10.017
6. Giovanini AF, de Sousa Passoni GN, Göhringer I, Deliberador TM, Zielak JC, Storrer CLM, et al. Prolonged use of alendronate alters the biology of cranial repair in estrogen-deficient rats' associated simultaneous immunohistochemical expression of TGF- β 1+, α -ER+, and BMPR1B. *Clin Oral Investig*. 2017; DOI: 10.1007/s00784-017-2292-y
7. Bosemark P, Isaksson H, Tägil M. Influence of systemic bisphosphonate treatment on mechanical properties of BMP-induced calluses in a rat fracture model: Comparison of three-point bending and twisting test. *J Orthop Res*. 2014;32(5):721-6. DOI: 10.1002/jor.22599

8. Gerstenfeld LC, Sacks DJ, Pelis M, Mason ZD, Graves DT, Barrero M, et al. Comparison of Effects of the Bisphosphonate Alendronate Versus the RANKL Inhibitor Denosumab on Murine Fracture Healing. *JBMR*. 2009;24(2):196-208. DOI: 10.1359/jbmr.081113
9. Triffitt JT. Initiation and enhancement of bone formation. A review. *Acta Orthop Scand*. 1987;58(6):673–84.
10. Sato M, Grasser W, Endo N, Akins R, Simmons H, Thompson DD, et al. Bisphosphonate action. Alendronate localization in rat bone and effects on osteoclast ultrastructure. *J Clin Invest*. 1991;88(6):2095–105. doi:10.1172/JCI115539.
11. Limirio PHJO, Rocha FS, Batista, JD, et al. The Effect of Local Delivery Doxycycline and Alendronate on Bone Repair. *AAPS PharmSciTech* 17, 872–877 (2016). DOI:10.1208/s12249-015-0411-0
12. Wang Z, Zhao Y, Zhang D, Qi B, Xiao W, Hu X, Yu A. A novel hybrid compound LLP2A-alendronate accelerates open fracture healing in a rabbit model. *Drug Des Devel Ther*.2019 Apr 5;13:1077-1086. DOI: 10.2147/DDDT.S195937.
13. Wang Y , Cui W , Zhao X , Wen S , Sun Y , Han J , Zhang H . Bone remodeling-inspired dual delivery electrospun nanofibers for promoting bone regeneration. *Nanoscale*.2018 Dec 20;11(1):60-71. DOI: 10.1039/c8nr07329e.
14. Leiblein, M., Henrich, D., Fervers, F. et al. Do antiosteoporotic drugs improve bone regeneration in vivo? *Eur J Trauma Emerg Surg* 46, 287–299 (2020). DOI:10.1007/s00068-019-01144-y
15. Deliberador FR, Sebastiani AM, Gerber JT, Bonetto L, Tórtora G, Giovanini AF et al. Effect of Local Application of Alendronate and Parathyroid Hormone on Craniofacial Bone Repair - a Preliminary Study. *Braz. Dent. J. [Internet]*. 2018 Sep; 29(5): 435-445. DOI: 10.1590/0103-6440201802120.
16. Weiss SG, Kuchar GO, Gerber JT, Tiboni F, Storrer CLM, Casagrande TC, et al. Dose of Alendronate directly increases trabeculae expansivity without altering bone volume in rat femurs. *World J Orthop*. 2018;9(10):190-7 DOI: 10.5312/wjo.v9.i10.203
17. Campos LD, Fornari JV, Bernabe AS, Leonardo MJ, Silva I, Arçari DP, et al. Comparação da Suplementação de Bifosfonato ou Vitamina D em Pacientes com Osteoporose ou Perda de Massa Óssea Induzida pelo uso de Glicocorticóides. *Saúde em Foco*. 2013;07:09-13.
18. Naruse K, Uchida K, Suto M, Miyagawa K, Kawata A, Urabe K, et al. Alendronate does not prevent long bone fragility in an inactive rat model. *J Bone Miner Metab*. 2015;online model:1-12. DOI: 10.1007/s00774-015-0714-y
19. Wermelin K, Suska F, Tengvall P, Thomsen P, Aspenberg P. Stainless steel screws coated with bisphosphonates gave stronger fixation and more surrounding bone. *Histomorphometry in rats. Bone*. 2008;42:365-71. DOI: 10.1016/j.bone.2007.10.013
20. Fu LJ, Tang TT, Hao YQ, Dai KR. Long-term effects of alendronate on fracture healing and bone remodeling of femoral shaft in ovariectomized rats. *Acta Pharmacol Sin* 2013;34:387-92. DOI: 10.1038/aps.2012.170
21. Spadaro JA, Damron TA, Horton JA, Margulies BS, Murray GM, Clemente DA, et al. Density and structural changes in the bone of growing rats after weekly alendronate administration with and

- without a methotrexate challenge. *J Orthop Res.* 2006;24(5):936-44. DOI: [10.1002/jor.20145](https://doi.org/10.1002/jor.20145)
22. [Apostu D](#), [Lucaciu O](#), [Mester A](#), [Oltean-Dan D](#), [Gheban D](#), [Rares Ciprian Benea H](#). Tibolone, alendronate, and simvastatin enhance implant osseointegration in a preclinical in vivo model. *Clin Oral Implants Res.* 2020 Apr 11. DOI: [10.1111/clr.13602](https://doi.org/10.1111/clr.13602).
 23. [Lee YS](#), [Gupta R](#), [Kwon JT](#), [Cho DC](#), [Seo YJ](#), [Seu SY](#), [Park EK](#), [Han I](#), [Kim CH](#), [Sung JK](#), [Kim KT](#). Effect of a bisphosphonate and selective estrogen receptor modulator on bone remodeling in streptozotocin-induced diabetes and ovariectomized rat model. *Spine J.* 2018 Oct;18(10):1877-1887. DOI: [10.1016/j.spinee.2018.05.020](https://doi.org/10.1016/j.spinee.2018.05.020).
 24. [Hauser M](#), [Siegrist M](#), [Denzer A](#), [Saulacic N](#), [Grosjean J](#), [Bohner M](#), [Hofstetter W](#). Bisphosphonates reduce biomaterial turnover in healing of critical-size rat femoral defects. *J Orthop Surg (Hong Kong)*. 2018 May-Aug;26(3):2309499018802487. DOI: [10.1177/2309499018802487](https://doi.org/10.1177/2309499018802487).
 25. [Lin JH](#), [Chen WI](#), [Duggan DE](#). Effects of dose, sex, and age on the disposition of alendronate, a potent antiosteolytic bisphosphonate, in rats. *Drug Metabolism and Disposition* July 1992, 20 (4) 473-478
 26. [Erlebacher A](#), [Filvaroff EH](#), [Ye J-Q](#), [Derynck R](#). Osteoblastic Responses to TGF β during Bone Remodeling. *Mol Biol Cell.* 1998;9:1903-18. DOI: [10.1091/mbc.9.7.1903](https://doi.org/10.1091/mbc.9.7.1903)
 27. [Bone H, Jr RD](#), [Tucci J](#). Dose-response relationships for alendronate treatment in osteoporotic elderly women. Alendronate Elderly Osteoporosis Study Centers. *Clin Endocrinol Metab.* 1997;82:265-74. DOI: [10.1210/jcem.82.1.3682](https://doi.org/10.1210/jcem.82.1.3682)
 28. [Seo J](#), [Yoo J](#), [Ryu J](#), [Yu K](#). Influence of Early Bisphosphonate Administration for Fracture Healing in Patients with Osteoporotic Proximal Humerus Fractures. *Clin Orthop Surg* 2016;8(4):437-43. DOI: [10.4055/cios.2016.8.4.437](https://doi.org/10.4055/cios.2016.8.4.437)
 29. [Li F](#), [Jiang P](#), [Pan J](#), [Liu C](#), [Zheng L](#). Synergistic Application of Platelet-Rich Fibrin and 1% Alendronate in Periodontal Bone Regeneration: A Meta-Analysis. *Biomed Res Int.* 2019 Aug 18; 2019:9148183. DOI: [10.1155/2019/9148183](https://doi.org/10.1155/2019/9148183).
 30. [Srisubut S](#), [Teerakapong A](#), [Vattraphodes T](#), [Taweekhaisupapong S](#). Effect of local delivery of alendronate on bone formation in bioactive glass grafting in rats. *Oral Surgery, Oral Medicine, Oral Pathology, Oral Radiology, and Endodontology.* 2007 Oct; 104(4): 11-16. DOI: [10.1016/j.tripleo.2007.04.022](https://doi.org/10.1016/j.tripleo.2007.04.022)
 31. [Wang Y](#), [Cui W](#), [Zhao X](#), [Wen S](#), [Sun Y](#), [Han J](#), [Zhang H](#). Bone remodeling-inspired dual delivery electrospun nanofibers for promoting bone regeneration. *Nanoscale.* 2018 Dec 20;11(1):60-71. DOI: [10.1039/c8nr07329e](https://doi.org/10.1039/c8nr07329e).
 32. [Özer T](#), [Aktas A](#), [Baris E](#), [Çelik HH](#), [Vatansever A](#). Effects of local alendronate administration on bone defect healing. Histomorphometric and radiological evaluation in a rabbit model. *Acta Cir Bras.* 2018 Sep;32(9):781-795. DOI: [10.1590/s0102-865020170090000010](https://doi.org/10.1590/s0102-865020170090000010).
 33. [Oliveira Nd](#), [Oliveira J](#), [Moraes LdS](#), [Weiss SG](#), [Chaves LH](#), [Casagrande TC](#), et al. Bone repair in craniofacial defects treated with different doses of alendronate: a histological, histomorphometric, and immunohistochemical study. *Clin Oral Investig.* 2018; DOI: [10.1007/s00784-018-2670-0](https://doi.org/10.1007/s00784-018-2670-0)

34. Chavarry NGM, Perrone D, Farias MLF, Dos Santos BC, Domingos AC, Schanaider A, Feres-Filho EJ. Alendronate improves bone density and type I collagen accumulation but increases the amount of pentosidine in the healing dental alveolus of ovariectomized rabbits. *Bone*.2019 Mar;120:9-19. DOI: 10.1016/j.bone.2018.09.022.
35. Miedel EL, Brisson BK , Hamilton T , Gleason H , Swain GP, Lopas L, Dopkin D, Perosky JE, Kozloff KM, Hankenson KD, Volk SW. Type III collagen modulates fracture callus bone formation and early remodeling *Journal of Orthopaedic Research* 2015 Volume 33, Issue 5 DOI: 10.1002/jor.22838
36. Isaac, C., Ladeira, P. R. S. d., Rêgo, F. M. P. d., Aldunate, J. C. B., e Ferreira, M. C. 2010. Processo de cura das feridas: cicatrização fisiológica *Rev Med (São Paulo)*, 89(3/4): 125-131
37. Ramchand SK, Seeman E. Reduced Bone Modeling and Unbalanced Bone Remodeling: Targets for Antiresorptive and Anabolic Therapy. *Handb Exp Pharmacol*.2020 Mar 31. DOI: 10.1007/164_2020_354.
38. Wan-Rong, B., Cai-Xia, J., Guo-Tong, X., e Chang-Qing, Y. 2013. Effect of alendronate sodium on the expression of mesenchymal-epithelial transition markers in mice with liver fibrosis. *Experimental and Therapeutic Medicine*, 5: 247-252.
39. Vieira JS, Cunha EJ, de Souza JF, Chaves LHK, de Souza JL, Giovanini AF. Alendronate disturbs femoral growth due to changes during immunolocalization of transforming growth factor- β 1 and bone morphogenetic protein-2 in epiphyseal plate. *World J Exp Med*. 2020 Jan 8;10(1):1-9. DOI: 10.5493/wjem.v10.i1.1.

Tables

Table I. Collagen levels among groups ($\times 10^6 \mu\text{m}^2$)

Note: One-way ANOVA, with significance level of 0.05.

Groups	Control	A1	A2
	Mean ± SD	Mean ± SD	Mean ± SD
Collagen I			
Absolute	4273.0 ± 859.7	3881.8 ± 860.4	3599.2 ± 592.3
Relative (%)	52.4	46.8	48.1
Collagen III			
Absolute	3881.9 ± 883.2	4398.4 ± 907.8	3875.8 ± 778.7
Relative (%)	47.6	56.75	51.9
Collagen (total)			
Absolute	8154.2 ± 1,432.2	8285.7 ± 1278.2	7475.0 ± 860.2

Table II. Internal and external measurements of the amount of bone trabeculae on the bone callus of the control group, A1, and A2 (pixels).

Note: Kruskal-Wallis, significance level of 0.05.

Measures in pixels (10^7)		
Groups	Internal callus	External callus
	Median (Min-max)	Median (Min-Max)
C	1.35 (1.12 – 1.55)	1.35 (0.85 – 1.53)
A1	1.39 (0.67 – 1.64)	1.28 (0.46 – 1.45)
A2	1.39 (1.14 – 1.64)	1.36 (1.03 – 1.52)
<i>p</i> value	0.785	0.598

Table III - Difference among the TGFβ-1 immunostaining groups in relation to the presence of chondroid matrix, bone matrix, and positivity for osteoblasts, hypertrophic cartilage, cartilage, and medullar area.

Note: (C) control group, (A1) 1mg/kg of alendronate group, and (A2) 2mg/kg of alendronate group. The symbol (+++) represents an intense immunostaining, (++) moderate immunostaining, and (+) poor immunostaining. The symbol (-) represents no immunostaining.

Groups	Presence of chondroid matrix	Presence of bone matrix	Osteoblast +	Hipertrofic Cartilage +	Cartilage + (rest/serial)	Medular area
C	++	+++	-	-	++	+++
A1	+++	++	-	+++	-	+
A2	++	+	-	.+	-	-

Figures

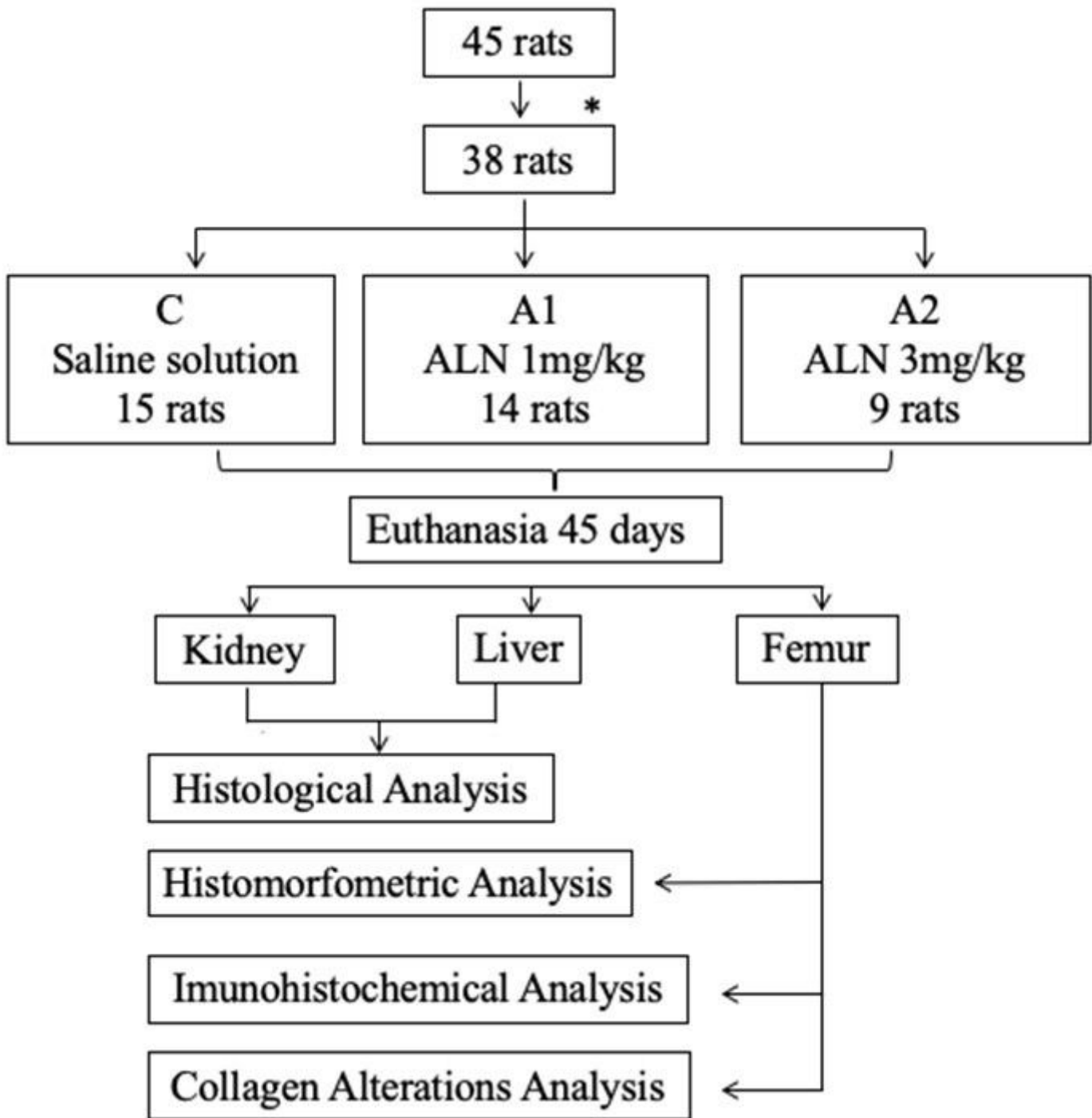


Figure 1

Fluxogram 1. Experimental design: 45 rats divided in control group, A1, and A2 Note: (*) denotes rats lost during surgery and experimental processing.

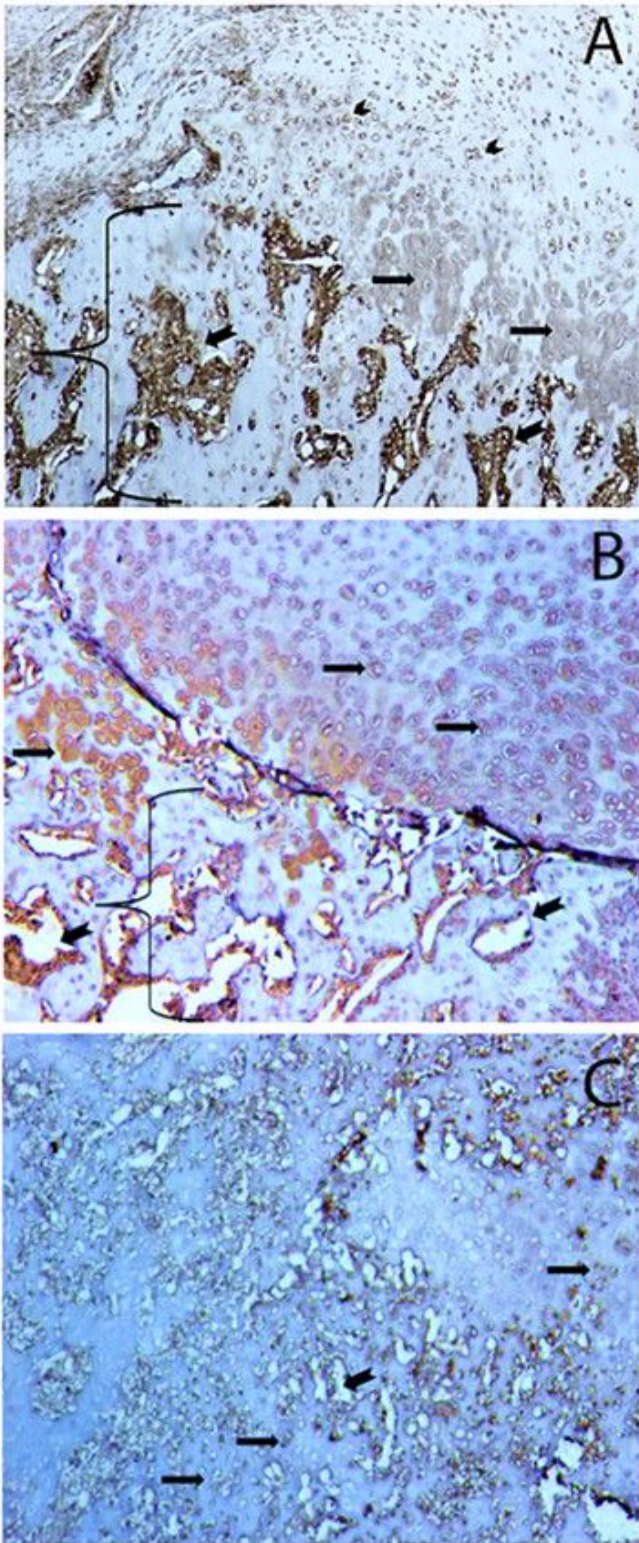


Figure 2

Micrographs of the immunoblotted slides with TGF β -1 marker at 100x magnification. Note: (A) Micrograph of control group; positive immunostaining in the medullary region (beveled arrow) of the area of bone formation (keys), marked in small chondrocytes (arrow), but negativity for hypertrophy (small arrow). (B) Micrograph of group A1; little positivity in the medullary region (beveled arrow) of the area of bone formation (keys), and advancement of the marking in the areas of hypertrophic cartilage (arrow).

(C) Micrograph of group A2; low positivity in the medullary region (beveled arrow) and fewer TGFβ-1 cells (arrow).

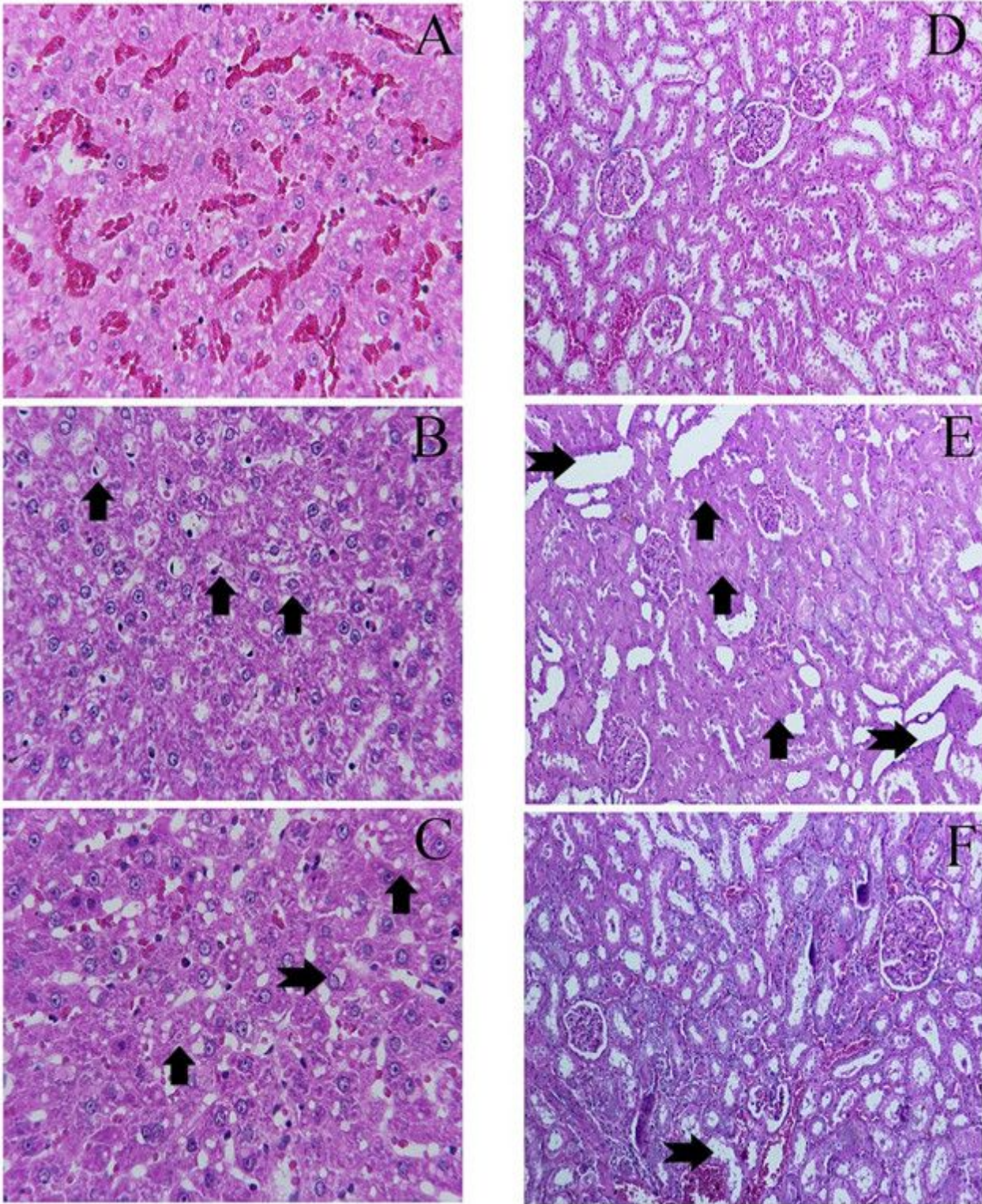


Figure 3

Liver and Kidney slices of groups C, A1, and A2 (HE - 100x). Note: Control group: histology of the liver with normal aspect (2A) and histology of the kidney with normal aspect (2D). Group A1: histology of the liver (2B) presenting cells with microguttular steatosis (arrow) and cells in signet ring. Kidneys (2E) showing

hyaline degeneration (arrow) and tubular ectasia (beveled arrow). Group A2: histology of the liver (2C) presenting cells with microgutticular steatosis (arrow) and cells in signet ring (beveled arrow). Kidneys (2F) presenting tubular ectasia (beveled arrow).

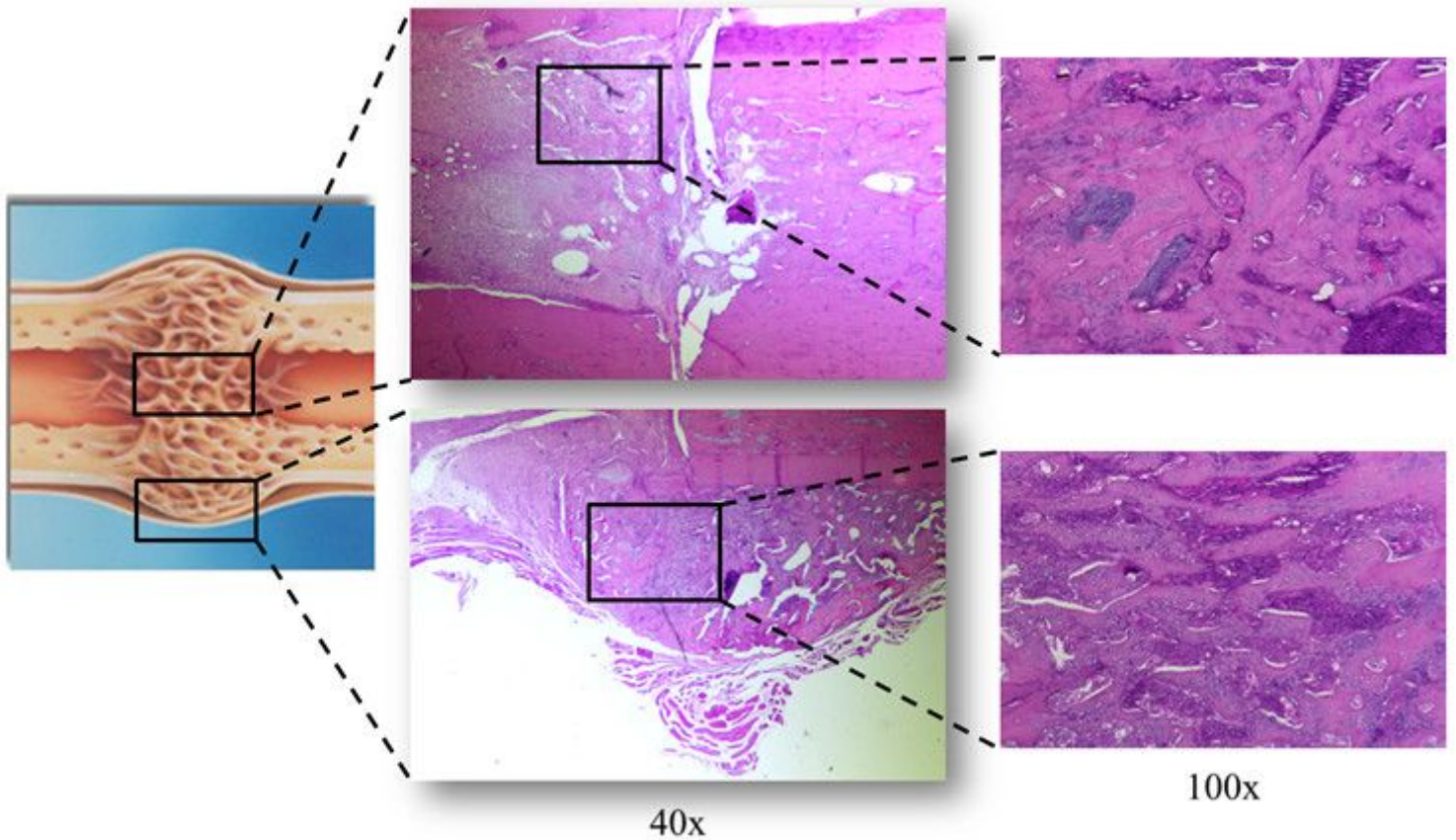


Figure 4

Histological area of bone trabeculation of internal (superior) and external (inferior) repair. Note: Increase by 40x and 100x (HE). Increased detail indicates the selected area of interest.

Supplementary Files

This is a list of supplementary files associated with this preprint. Click to download.

- [coverletterBMC.docx](#)
- [ARRIVEIngles.pdf](#)